Acta Biomaterialia 48 (2017) 468–478

Contents lists available at ScienceDirect

Acta Biomaterialia

journal homepage: www.elsevier.com/locate/actabiomat

Full length article

In vitro degradation kinetics of pure PLA and Mg/PLA composite: Effects of immersion temperature and compression stress

Xuan Li [a,b], Chenglin Chu [a,b,*], Yalin Wei [a,b], Chenxi Qi [a,b], Jing Bai [a,b], Chao Guo [a,b], Feng Xue [a,b], Pinghua Lin [a,b], Paul K. Chu [c]

[a] *School of Materials Science and Engineering, Southeast University, Nanjing 211189, China*
[b] *Jiangsu Key Laboratory for Advanced Metallic Materials, Southeast University, Nanjing 211189, China*
[c] *Department of Physics and Materials Science, City University of Hong Kong, Tat Chee Avenue, Kowloon, Hong Kong, China*

A R T I C L E I N F O

Article history:
Received 25 May 2016
Received in revised form 25 October 2016
Accepted 1 November 2016
Available online 2 November 2016

Keywords:
Degradation kinetics
Magnesium-based fillers
Poly-lactic acid
Compression stress
Bending strength

A B S T R A C T

The effects of the immersion temperature and compression stress on the *in vitro* degradation behavior of pure poly-lactic acid (pure-PLA) and PLA-based composite unidirectionally reinforced with micro-arc oxidized magnesium alloy wires (Mg/PLA or MAO-MAWs/PLA) are investigated. The degradation kinetics of pure-PLA and the PLA matrix in MAO-MAWs/PLA exhibit an Arrhenius-type behavior. For the composite, the synergic degradation of MAO-MAWs maintains a steady pH and mitigates the degradation of PLA matrix during immersion. However, the external compression stress decreases the activation energy (E_a) and pre-exponential factor (k_0) consequently increasing the degradation rate of PLA. Under a compression stress of 1 MPa, E_a and k_0 of pure PLA are 57.54 kJ/mol and 9.74×10^7 day^{-1}, respectively, but 65.5 kJ/mol and 9.81×10^8 day^{-1} for the PLA matrix in the composite. Accelerated tests are conducted in rising immersion temperature in order to shorten the experimental time. Our analysis indicates there are well-defined relationships between the bending strength of the specimens and the PLA molecular weight during immersion, which are independent of the degradation temperature and external compression stress. Finally, a numerical model is established to elucidate the relationship of bending strength, the PLA molecular weight, activation energy, immersion time and temperature.

Statement of significance

We systematically evaluate the effects of compression stress and temperature on the degradation properties of two materials: (pure-PLA) and MAO-MAWs/PLA (or Mg/PLA). The initial *in vitro* degradation kinetics of the unstressed or stressed pure-PLA and MAO-MAWs/PLA composite is confirmed to be Arrhenius-like. MAO-MAWs and external compression stress would influence the degradation activation energy (E_a) and pre-exponential factor (k_0) of PLA, and we noticed there is a linear relationship between E_a and ln k_0. Thereafter, we noticed that Mg^{2+}, not H^+, plays a significant role on the mitigation of the PLA degradation and external compression stress brings the molecular structure change of PLA. Finally, we proposed a model to predict the bending strength of the specimens versus immersion time at different immersion temperatures. This fundamental study could provide some scientific basis in our understanding for the evaluations and biomedical applications of these biodegradable materials.

1. Introduction

Biodegradable polymers are desirable for orthopedic fixation implants, sutures and drug delivery [1–5]. However, most biopolymers are aliphatic polyesters which usually possess poor mechanical properties and release acidic degradation products which may cause premature implant failure and local inflammation [6,7]. In order to overcome these hurdles, magnesium-based fillers (Mg fillers) which are themselves biodegradable can be incorporated into biodegradable polymers [8–11]. In biomedical applications, an important property is the load-bearing ability under external loading, and the implants must have sufficient mechanical integrity until tissues heal, typically 5–12 weeks for bones [12].

---

* Corresponding author at: School of Materials Science and Engineering, Southeast University, Nanjing 211189, China.
E-mail address: clchu@seu.edu.cn (C. Chu).

http://dx.doi.org/10.1016/j.actbio.2016.11.001

Despite recent advances in magnesium/polymer composites [8–11,13,14], some mechanisms are still not fully understood. The first one is the effect of Mg fillers on the degradation kinetics of biodegradable polymers. The degradation kinetics of aliphatic biopolymers have been widely investigated and the generally accepted theory is third-order kinetics [15–17] which stipulates that the degradation rate depends on the concentration of the polymer bonds and acidic degradation products. The Mg fillers affect the pH decrease and alter hydrolytic degradation of the polymers [9,13,14,18]. In order to tailor the degradation rate, it is necessary to fully understand the role of Mg fillers on the degradation kinetics of biopolymers. The second one is the quantitative effect of the immersion temperatures on the degradation properties. Some polymers may degrade for more than 3 years [19,20]. In order to shorten the experimental time and cost, accelerated tests are frequently performed at an elevated immersion temperature. *In vivo*, the implants should depict sufficient mechanical performance at least until the healing of tissues. Hence, to reflect the mechanical integrity in this period by the accelerated tests, it is important to establish the correlation between normal and accelerated tests. The third one is the role of external compression stress. For example, tensile stress has been shown to increase the degradation rate of biopolymers [21,22] and Guo et al. [22] have shown degradation of biodegradable poly(L-lactide-co-glycolide) (PLGA) is related to the loading magnitude. In the tensile stress ranges between 0.1 MPa and 0.5 MPa, a higher tensile stress leads to faster degradation. However, Deng et al. [23] have observed that the tensile loads have no effect on the degradation of PGLA (90/10 poly (glycolide-co-L-lactide). This discrepancy suggests that it is necessary to study the effects of external stress on the degradation behavior systematically. In addition to tensile stress, compression stress is a normal physiological stress mode and plays a significant role in human bone metabolism *in vivo* [24–26]. Therefore, it is also important to investigate the influence of external compression stress on the degradation behavior. The fourth one is concerned with the relationship between mechanical properties and the molecular weight of biopolymers, immersion time, and external conditions such as external stress and temperature. Deng et al. have observed a linear relationship between the tensile strength of poly(glycolide-co-L-lactic) and logarithmic molecular weight [23] but it is not clear if a similar relationship exists for stressed specimens.

In this work, poly-lactic acid (PLA) based composite unidirectionally reinforced with micro-arc oxidized magnesium alloy wires (Mg/PLA or MAO-MAWs/PLA) is prepared. The role of Mg on the degradation kinetic of PLA is investigated by immersion tests. Accelerated tests are conducted to quantitatively evaluate the effect of the immersion temperature on the degradation properties of pure poly-lactic acid (pure-PLA) and the composite. Thereafter, effects of external compression stress on the degradation behaviors of pure-PLA and the composite are studied and the relationships between the bending strength, molecular weight of PLA, external stress and temperature for pure-PLA and the composite are discussed. The main purpose is to provide some scientific basis for the design and evaluation of Mg/PLA composite.

2. Materials and methods

2.1. Materials preparation

The PLA particles with a density and glass transition temperature of 1.24 g/cm^3 and 65 °C, respectively, were purchased from Natureworks LLC. The MAWs composed of AZ31 (96% Mg, 3% Al and 1% Zn by weight) with a diameter of 0.3 mm were fabricated by continuous smelting, casting, hot extrusion, wet drawing, and annealing. Afterwards, the MAWs underwent micro-arc oxidization (MAO-MAWs) on the WHD-30 type MAO equipment [27]. The main composition of MAO coating is MgO and its surface flatness and porosity is respectively about 67% and 9.2% calculated by the method mentioned in the other literature [27]. The composite with MAO-MAWs and PLA (MAO-MAWs/PLA) was prepared using a stack-heat-compressing process described in our previous paper [8]. The volume fraction of MAO-MAWs in the composite was 10 vol%.

2.2. In vitro tests

Kirkland's biocorrosion media (KBM) [28] with a pH 7.4 at 37 °C was used as the immersion fluid and the composition is shown in Table 1. The dimensions of the immersion samples were 50 mm × 12 mm × 2 mm. The ratios of the solution in milliliters to specimen weight (grams) and surface area (square centimeters) were larger than 30:1 and 50:1, respectively. The immersion fluid was changed every day and prior to the change, the pH was measured. *In vivo*, the bone healing times for fractures are typically 5–12 weeks [12]. In this work, the immersion times were approximately selected as 1, 2, 3 and 4 weeks to represent the early stage of the bone healing. The long term performance would be discussed with the results represented in our previous work after 8 weeks immersion [8].

Three sets of temperature (25 °C, 37 °C, and 50 °C) below the glass transition temperature were selected to evaluate the influence of immersion temperature on materials degradation. To investigate the dependence of the external compression stress on degradation, a stress load of 1 MPa was applied to the samples as shown in Fig. 1. In order to prevent partial bending during immersion, the main part of the specimen was fixed with honeycombed polytetrafluoroethylene. Three specimens were tested for each parameter and the averages were used in the assessment.

The viscosity average molecular weight (M_v) of PLA was calculated by the Mark-Houwink-Sakurada formula [29] based on the intrinsic viscosity at 25 °C monitored by the Ubbelohde viscometer. The mass loss ratio (ω) was calculated by the following equation:

$$\omega = ((m_0 - m_t)/m_0) \times 100\% \qquad (1)$$

where m_0 is the initial mass and m_t is the final mass of the specimen after immersion after drying for 48 h in an oven at 37 °C.

2.3. Mechanical tests

The bending tests were conducted on the CMT4503 electronic universal testing machine at room temperature at a crosshead speed of 2 mm/min. The bending strength (S_b) of the wet samples was determined by the three-point bending method according to the standard ASTMD790-2010 for a span of 32 mm.

Table 1
Composition of KBM [28].

Component	Human plasma (mmol/L)	KBM (mmol/L)
Na^+	142	120.3
Cl^-	103	102.5
K^+	5.0	5.0
Ca^{2+}	2.5	2.5
Mg^{2+}	1.5	1.5
HPO_4^{2-}	1	0.9
SO_4^{2-}	0.5	0.5
D-Glucose	5	5
HEPES	–	25

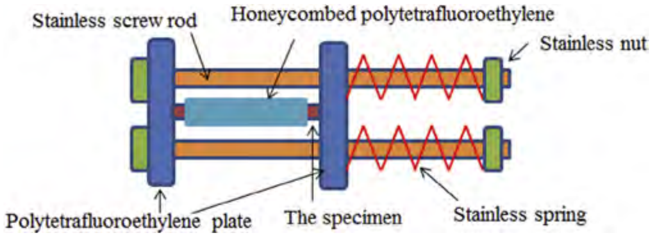

Fig. 1. Schematic illustration of the setup to apply the compression stress. The stainless spring controls the stress load and the honeycomb polytetrafluoroethylene prevents the sample from partial bending while allowing the fluid to immerse the specimen.

2.4. Microstructural characterization

Scanning electron microscopy (SEM) was performed on the Philips XL30 FEG an accelerating voltage of 20–25 kV to examine the morphology of the MAWs during immersion. The specimens were mounted on a stub and sputter-deposited with a thin gold layer in argon.

2.5. Statistical analysis

Experimental data was statistically analyzed and is presented as average of three measurements along with the standard deviation wherever possible. The analysis of variance was used to determine the statistical significance of the results with $p = 0.05$. In addition, the experimental data was also curve fitted by least-squares fitting whenever possible. The associated error of the correlation results was estimated by the propagation of error for the parameters of the fitted curves. The statistical software Origin (OriginLab Corporation, Northampton, USA) was used for data analysis.

3. Results and discussion

3.1. Degradation kinetics of the unstressed pure-PLA and MAO-MAWs/PLA

3.1.1. Degradation behavior

The pH changes in the fluids during immersion at 37 °C are displayed in Fig. 2(a). In the first 10 days, the pH changes slightly for both pure-PLA and MAO-MAWs/PLA. Thereafter, the pH decreases gradually for pure-PLA but remains constant for the composite, suggesting that MAO-MAWs mitigate the pH decrease arising from the degradation of PLA. The mass loss ratio (ω) of the specimens during immersion are shown in Fig. 2(b). After immersion for 30 days, ω is 1.15% and 1.45% for pure-PLA and the composite, respectively. A larger ω of the composite indicates that MAO-MAWs degrade during immersion.

It has been reported PLA follows the first order degradation during initial immersion [15,16]. The relationship between logarithmic M_v of PLA and immersion time is shown in Fig. 2(c). A linear relationship is observed suggesting that the PLA matrix in the composite follows the first-order degradation in the predetermined immersion time. Here, ln M_v as the function of immersion time (t) can be described as follows:

$$\ln M_v = A - k \times t \tag{2}$$

where A is a constant value and k is the degradation rate. Curve fitting yields A and k of 11.133 g·mol^{-1} and 0.0103 g·mol^{-1}·day^{-1},

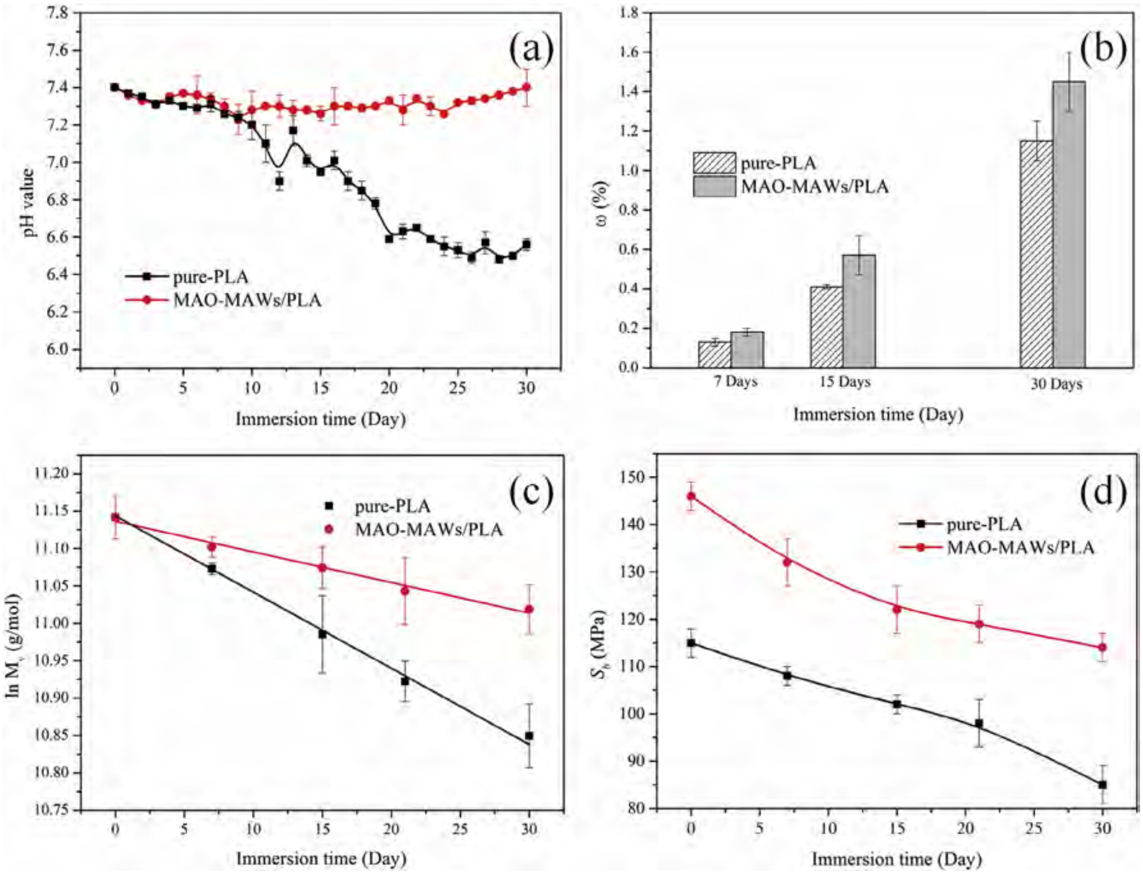

Fig. 2. Degradation behavior of pure-PLA and MAO-MAWs/PLA during immersion at 37 °C: (a) pH changes in the fluid; (b) ω changes; (c) ln M_v versus immersion time; (d) S_b changes versus immersion time.

respectively, for pure-PLA and 11.136 $g{\cdot}mol^{-1}$ and 0.0041 $g{\cdot}mol^{-1}{\cdot}day^{-1}$ for the PLA matrix in the composite. The PLA in the composite has a lower degradation rate than that of pure-PLA. The bending strength (S_b) changes with immersion time as shown in Fig. 2(d). The initial S_b of pure-PLA and the composite is 115 MPa and 146 MPa, respectively. After immersion for 30 days, it decreases to 85 MPa and 115 MPa, respectively, corresponding to 0.26 and 0.21 times reduction. The composite has better strength retention ability.

3.1.2. Effects of immersion temperature on the degradation behavior

The effects of temperature on the pH and ω changes are presented in Fig. 3. A high immersion temperature decreases the pH for pure-PLA but increases the pH for the composite. This is further confirmed by the ω changes. After immersion for 15 days, ω for pure-PLA and the composite is 0.56% and 0.88% at 50 °C, respectively, and larger than the values of 0.33% and 0.4% at 25 °C. After immersion, the PLA matrix was dissolved in chloroform and the surface morphology of the MAO-MAWs in the composite is shown in Fig. 4. Rising immersion temperature would deteriorate the surface breakage of MAO-MAWs, consisting with theω changes.

3.1.3. Degradation kinetics

If the temperature dependence of the degradation rate follows an Arrhenius-type equation, k in Eq. (2) can be expressed as

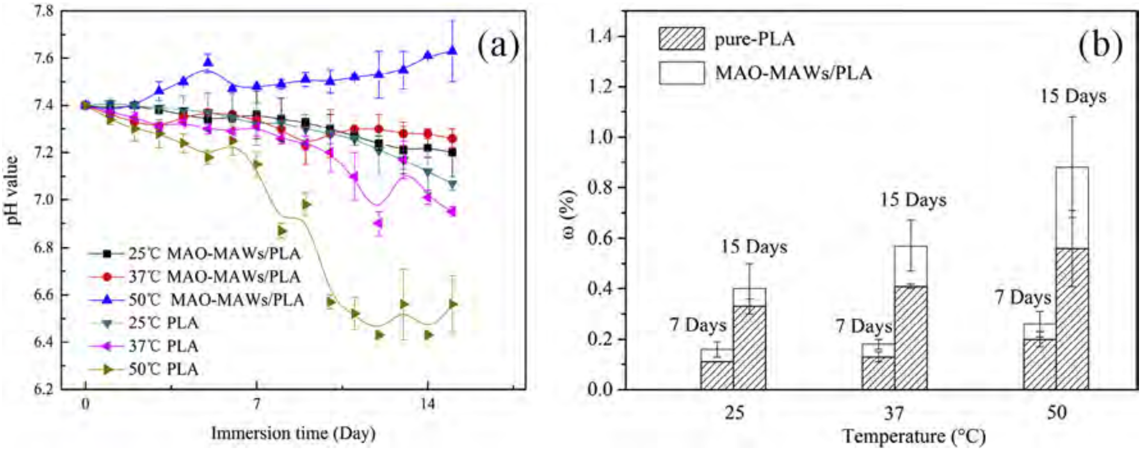

Fig. 3. (a) pH changes in the immersion fluid and (b) ω changes of the specimens as a function of immersion time and temperature.

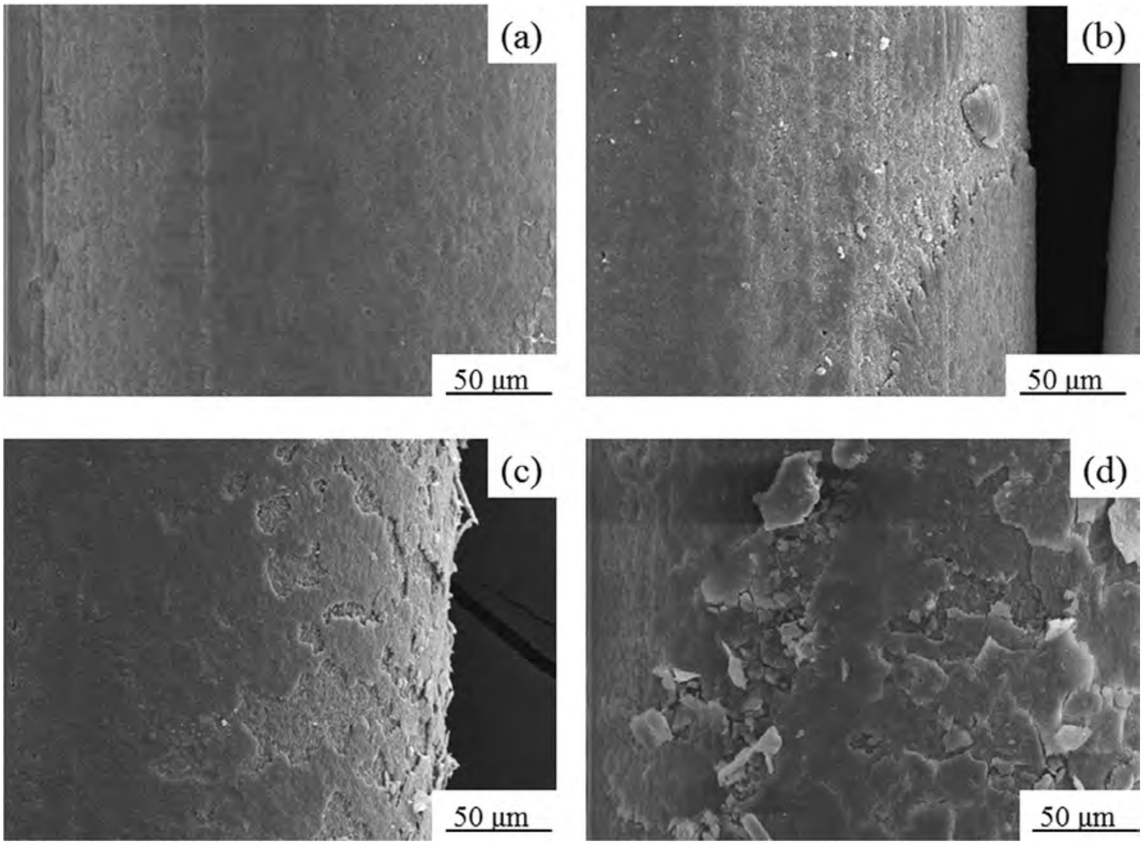

Fig. 4. Surface morphology of the MAO-MAWs in the composite after immersion for 15 days at different immersion temperature: (a) Initial morphology, (b) 25 °C, (c) 37 °C, and (d) 50 °C.

$$k = k_0 exp(-E_a/RT) \tag{3}$$

where k_0 is pre-exponential factor, E_a is activation energy, R is gas constant, and T is temperature. Dividing Eq. (3) by Eq. (2) produces a linear relationship between ln(A-ln M_v) and 1/T. The results after immersion for 7 days are shown in Fig. 5(a). By means of curve fitting, k_0 and E_a are 2.17×10^{11} day^{-1} and 79.52 kJ/mol, respectively, for pure-PLA and 1.16×10^{13} day^{-1} and 91.15 kJ/mol for the PLA matrix in the composite. The E_a is a little smaller than the results from the study by Deng [23]. The curves of M_v versus immersion time for the pure-PLA and PLA matrix in the composite based on Eqs. (2) and (3) are illustrated in Fig. 5(b) and (c), respectively. The simulated values after immersion for 15 days at different temperature agree with the experimental ones. Moreover, the PLA matrix in the composite has larger E_a and k_0 than pure-PLA, suggesting that the MAO-MAWs influence the degradation kinetics of PLA by changing not only the activation energy but also the pre-exponential factor.

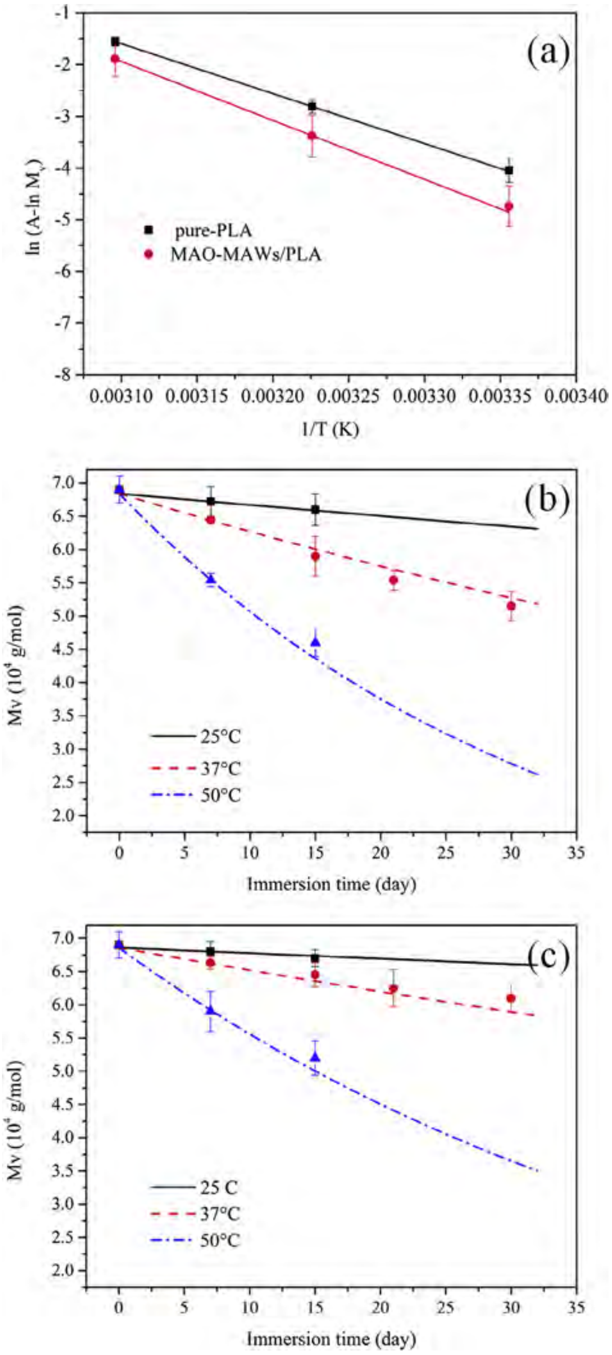

Fig. 5. Relationship between M_v and immersion temperature with immersion time: (a) ln (A-ln M_v) as a function of 1/T after immersion for 7 days; (b) M_v of pure-PLA as a function of immersion time at different temperature; (c) M_v of the PLA matrix in the composite as a function of immersion time at different temperature.

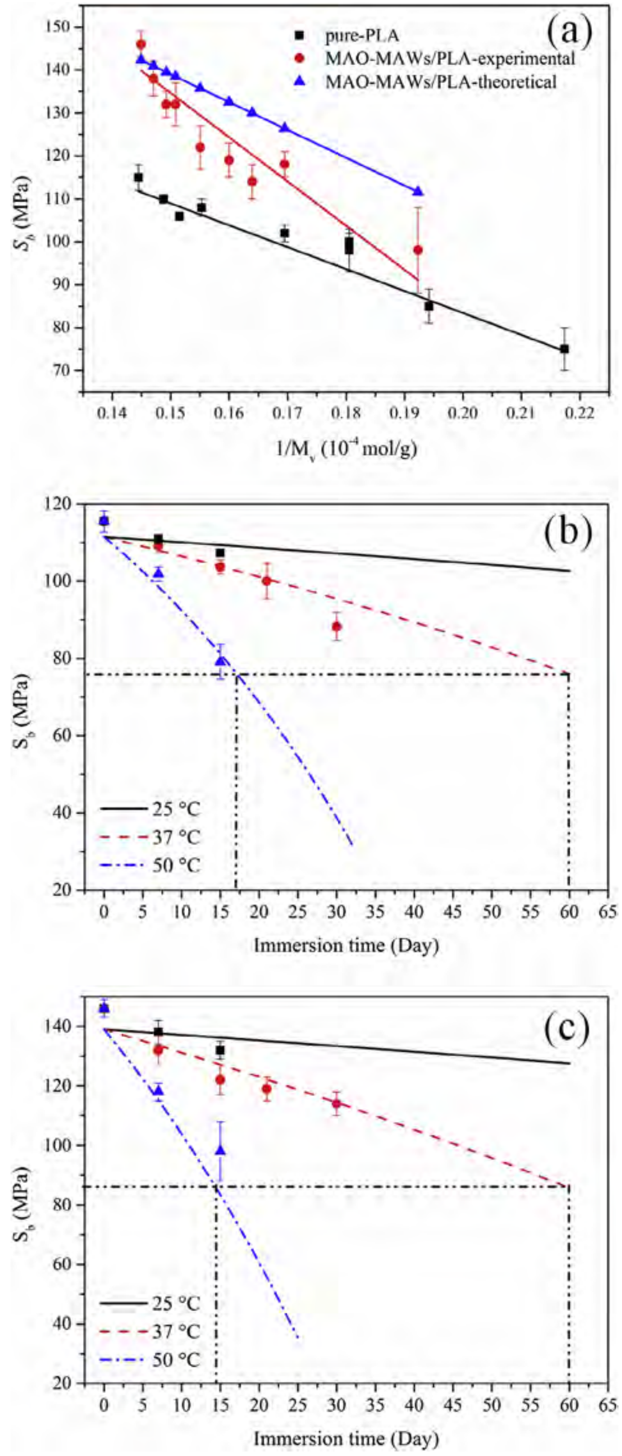

Fig. 6. Relationship between the bending strength, molecular weight of PLA, temperature, and immersion time: (a) S_b as a function of $1/M_v$; (b) S_b of pure-PLA as a function of immersion time at different immersion temperature; (c) S_b of the composite as a function of immersion time at different immersion temperature.

3.1.4. Relationship between bending strength and PLA molecular weight

The bending strength is a critical factor and for biodegradable polymers, it decreases gradually *in vitro*. The relationship between the fracture strength σ_s and molecular weight (M_n) of the polymer is represented as follows [30]:

$$\sigma_s = \sigma_{s\infty} - B/M_n, \tag{4}$$

where $\sigma_{s\infty}$ is the fracture strength at a finite molecular weight and B is a constant value. It has been reported that the ratio of the strength between pure bending and pure tension for brittle materials obeys the Weibull theory and depends on the volume of the specimen and Weibull modulus [31]. If Eq. (4) is applicable, one would get a linear curve by plotting S_b vs. $1/M_v$. According to Fig. 6(a), the experimental S_b for pure-PLA and the composite shows a linear relationship to $1/M_v$. The relationship between the bending strength and molecular weight of PLA is shown in the following:

$$S_b = S_{b\infty} - B/M_v, \tag{5}$$

where $S_{b\infty}$ is the bending strength at finite molecular weight. By means of curve fitting, $S_{b\infty}$ and B are 186 MPa and 5.1 × 10^6 MPa·g/-mol, respectively for pure-PLA and 289 MPa and 1.029 × 10^7 MPa·g/mol for the composite. Since the data are acquired at all three temperatures, the relationship is independent of the immersion temperature. Changes of the MAWs distribution influence S_b, probably resulting in poorer linear fitting for the composite than pure-PLA. The relationship between the initial bending strength of the composite ($S_{b\text{-}composite}$) and PLA ($S_{b\text{-}PLA}$) with the same dimensions could be described as follows [8]:

$$S_{b-composite} = S_{b-PLA} I_{z-composite}/I_{z-pure-PLA} \tag{6}$$

where $I_{z\text{-}composite}$ is the equivalent inertia moment of the composite, and $I_{z\text{-}pure\text{-}PLA}$ is the equivalent inertia moment of pure-PLA. The ratio of $I_{z\text{-}composite}$ to $I_{z\text{-}pure\text{-}PLA}$ could be calculated to be 1.27 in this work. Then, $S_{b\infty}$ and B for the composites can be calculated as follows:

$$S_{b\infty-composite} = S_{b\infty-pure-PLA} I_{z-composite}/I_{z-pure-PLA} \tag{7}$$

$$B_{composite} = B_{pure-PLA} I_{z-composite}/I_{z-pure-PLA} \tag{8}$$

where $S_{b\infty\text{-}pure\text{-}PLA}$ is $S_{b\infty}$ of the pure-PLA and $B_{pure\text{-}PLA}$ is B of pure-PLA. The theoretical results based on Eqs. (7) and (8) for the composite versus $1/M_v$ are calculated and shown in Fig. 6(a). The theoretical results are a little larger than those of the experimental ones and the difference would be more pronounced for lower M_v. This may be attributed to the gradually decreased interface adhesion properties between MAO-MAWs and PLA matrix during immersion.

The evolution of S_b versus immersion time at different immersion temperatures based on Eqs. (2), (3), and (5) is illustrated in Fig. 6(b) and (c). The simulated results match the experimental ones and the relationship between accelerated and normal tests can be obtained. The corresponding immersion time for the accelerated test at 50 °C to reflect the normal 2 month degradation at 37 °C is 17 days and 15 days, respectively, for the pure-PLA and the composite. The results are similar to those in another study [8], suggesting accelerated tests at a high temperature are valid and can indeed shorten the experimental time.

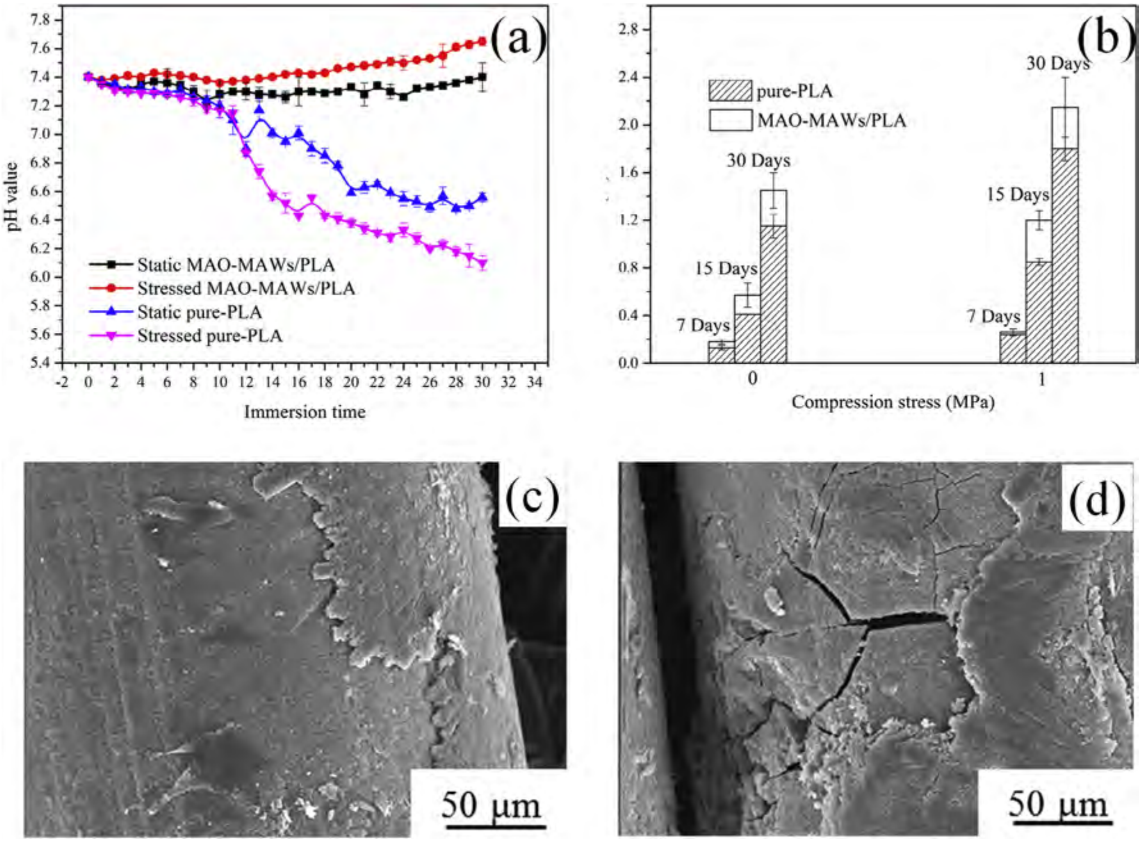

Fig. 7. Degradation behavior of the stressed specimens immersed at 37 °C: (a) pH changes in the immersion fluids versus immersion time; (b) ω changes of the specimens; (c) surface morphology of MAO-MAW in the unstressed composite after immersion for 30 days; (d) surface morphology of MAO-MAW in the stressed composite after immersion for 30 days.

3.2. Degradation kinetics of the stressed pure PLA and MAO-MAWs/PLA

3.2.1. Degradation behavior

As shown in Fig. 7(a), a smaller pH and larger higher pH is observed from the stressed pure-PLA and composite during immersion at 37 °C, respectively, compared to the unstressed specimens. After immersion for 30 days, ω for the stressed pure-PLA and composite is 1.8% and 2.15%, respectively, and 1.15% and 1.45% for the unstressed specimens. The surface morphology of the MAO-MAWs in the unstressed and stressed composite after immersion for 30 days at 37 °C is depicted in Fig. 7(c) and (d), respectively. The MAO-MAWs show cracks under the unstressed condition and the MAW substrate experiences critical breakage under the stressed condition. The results suggest that compression stress simultaneously enhances the degradation of PLA matrix and MAO-MAWs. The effects of compression stress on the degradation of PLA agree with those reported earlier for external tensile loading [21,22], but disagree with the study on photodegradation of the polymer, in which compressive stress is found to retard the rate of chain scission [32], implying that the effects of compression stress on degradation may be quite complicated.

3.2.2. Effects of immersion temperature on the degradation behavior

The temperature effects on the degradation behavior of the stressed specimens are show in Fig. 8. A high temperature decreases the pH for pure-PLA but increases the pH for the composite. After immersion for 15 days at 50 °C, the pH of the solution for the stressed pure-PLA and composite is 6.2 and 7.9, respectively, compared to 6.5 and 7.6 for the unstressed specimens. Meanwhile, ω for the stressed pure-PLA and composite is 1.0% and 1.4%, respectively, and 0.5% and 0.8% for the unstressed specimens. The combined effects of external compression stress and temperature promote degradation of the pure-PLA and composite and are more pronounced for longer immersion time.

3.2.3. Degradation kinetics

The degradation kinetics of the specimens under compression stress of 1 MPa is studied by the same method as the unstressed ones. The calculated E_a and k_0 for the stressed specimens are illustrated in Table 2. Using these values, the simulated curves of M_v for the stressed specimens as a function of immersion time at different temperature are shown in Fig. 9(a) and (b). The simulated results are consistent with the experimental ones, suggesting that the degradation kinetics of the stressed pure-PLA and PLA matrix in the composite is Arrhenius-like. Additionally, the external compression stress decreases E_a and k_0.

Table 2
E_a and k_0 of the pure-PLA and PLA matrix in the composite under unstressed and stressed conditions.

	E_a (kJ/mol)	k_0 (day^{-1})
Unstressed pure-PLA	79.52 (±0.45)	$(2.17 \pm 0.01) \times 10^{11}$
Stressed pure-PLA	57.54 (±3.01)	$(9.74 \pm 0.59) \times 10^{7}$
Unstressed MAO-MAWs/PLA	91.15 (±2.23)	$(1.16 \pm 0.007) \times 10^{13}$
Stressed MAO-MAWs/PLA	65.5 (±4.13)	$(9.81 \pm 0.69) \times 10^{8}$

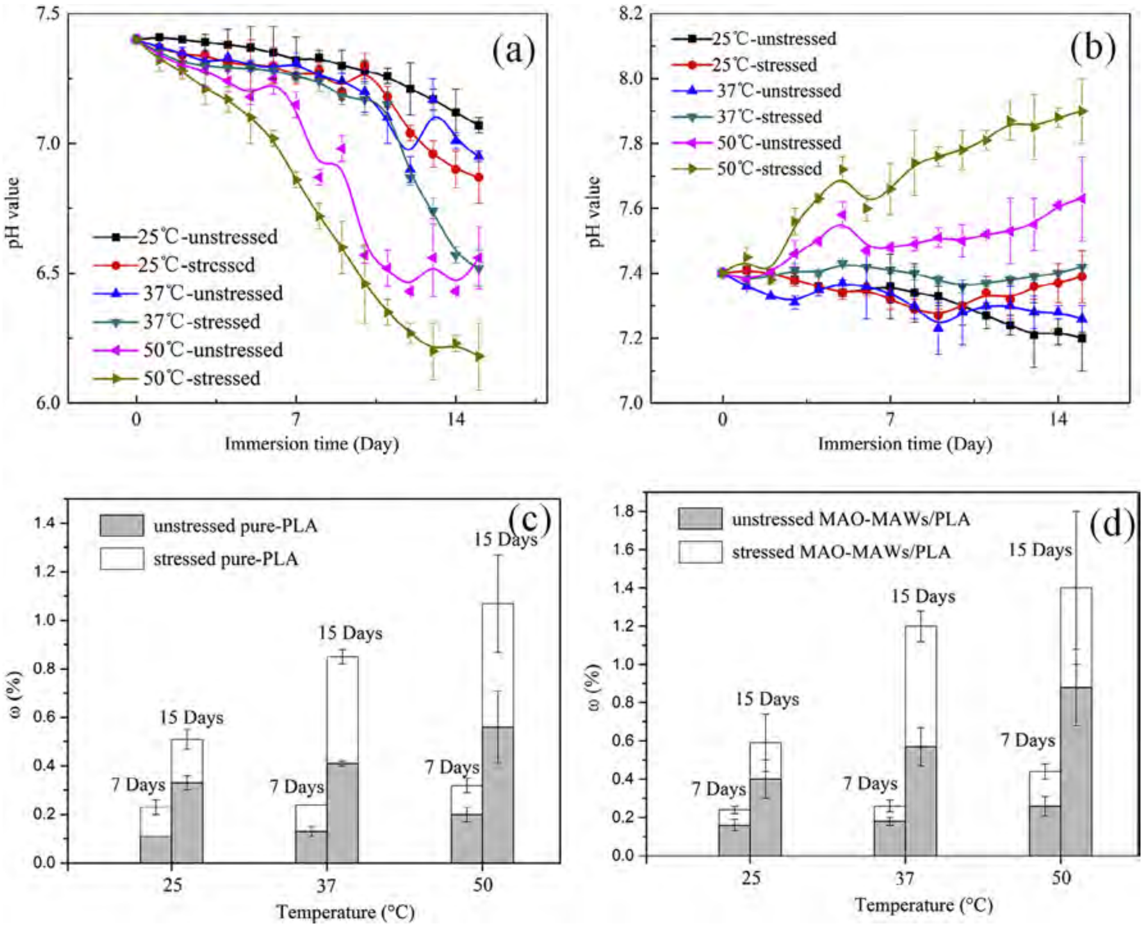

Fig. 8. Degradation behavior of the stressed specimens as a function of immersion temperature and time: (a) pH changes in immersion fluid for pure-PLA; (b) pH changes in the immersion fluid for the composite; (c) ω changes of pure-PLA; (d) ω changes of the composite .

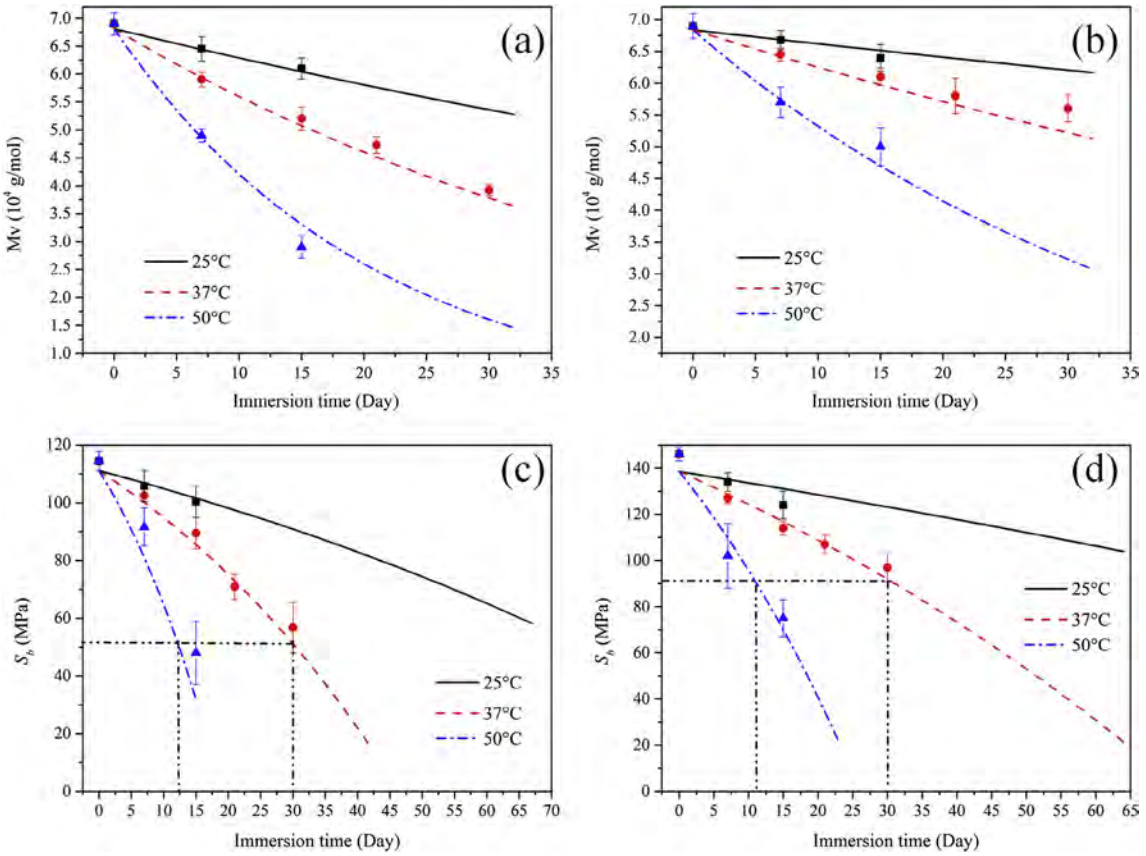

Fig. 9. Relationship between the bending strength, molecular weight of PLA, immersion time, and temperature of stressed specimens: (a) M_v of stressed pure-PLA as a function of immersion time at different immersion temperature; (b) M_v of PLA matrix in the stressed composite as a function of immersion time at different immersion temperature; (c) S_b of stressed pure-PLA as a function of immersion time at different immersion temperature; (d) S_b of the stressed composite as a function of immersion time at different immersion temperature.

The simulated curves of S_b for the stressed specimens as a function of immersion time are shown in Fig. 9(c) and (d) and agree well with the experimental data, indicating that the relationship between bending strength and molecular weight of PLA is independent of the external compression stress. The stressed pure-PLA loses its bending strength no more than 60 days during normal immersion at 37 °C. Application of external compression stress seems to change the correlation between the accelerated tests and normal tests. To reflect 30 days normal immersion at 37 °C, the corresponding accelerated immersion time at 50 °C for the stressed pure-PLA and composite is about 12 days and 11 days, respectively, and 9 days and 7 days for the unstressed specimens.

3.3. Discussions on degradation kinetics

3.3.1. Relationship between activation energy and pre-exponential factor

It is clear that k_0 is not a constant for PLA and increases with E_a. Moreover, a linear correlation between $\ln k_0$ and E_a exists as shown in Fig. 10(a). This relationship obeys the Meyer–Neldel rule or compensation law [33,34] and the relationship between E_a and k_0 can be described by the following equation:

$$\ln k_0 = a + b \times E_a \tag{9}$$

where a and b are -2.16 and 3.54×10^{-1} mol/kJ, respectively. The compensation effect has been noticed in a series of solid acid-catalysed reactions [35,36] and the electrical conductivity of semiconducting materials [34,37]. It is believed this effect is due to the compensation between the activation entropy and the activation enthalpy. Recently, a study performed by Huang et al. [38] suggests there is also a compensation effect for the pyrolysis of poly(L-lactide) (PLLA), which was considered to be induced by the change in reactant properties. The compensation effect for *in vitro* degradation of PLA in this work is the first time in our understanding to be reported. Based on Eqs. (3), (9), and Eq. (2), the relationship between M_v, temperature, immersion time, and activation energy is as follows:

$$M_v = \exp(A - \exp(a + b \times E_a) \times t \times \exp(-E_a/RT)) \tag{10}$$

According to Eq. (10), the curves of M_v for PLA versus immersion time during normal degradation (37 °C) in Fig. 10(b) fit the experimental results and limiting decrease in M_v is observed when E_a is 0. The changes in S_b for pure-PLA and the composite versus immersion time at 37 °C under this limiting condition are shown in Fig. 10(c), showing that pure-PLA and the composite quickly lose the mechanical properties in less than 9 days.

3.3.2. Synergic degradation effects of Mg fillers in the composite

Apparently, MAO-MAWs could maintain pH a steady value during the normal degradation tests. It is well known that the main degradation mechanism of aliphatic polyesters is hydrolysis which involves hydrolytic cleavage of the ester linkage to produce hydrophilic groups. During the degradation, the acidic degradation products would release acidic ions and reduce pH. The low pH could form the acidic environment near the implants and probably cause bone resorption or local inflammation [39,40]. In opposition to aliphatic polyesters, the degradation of basic MAO coating or Mg releases hydroxide ions. This

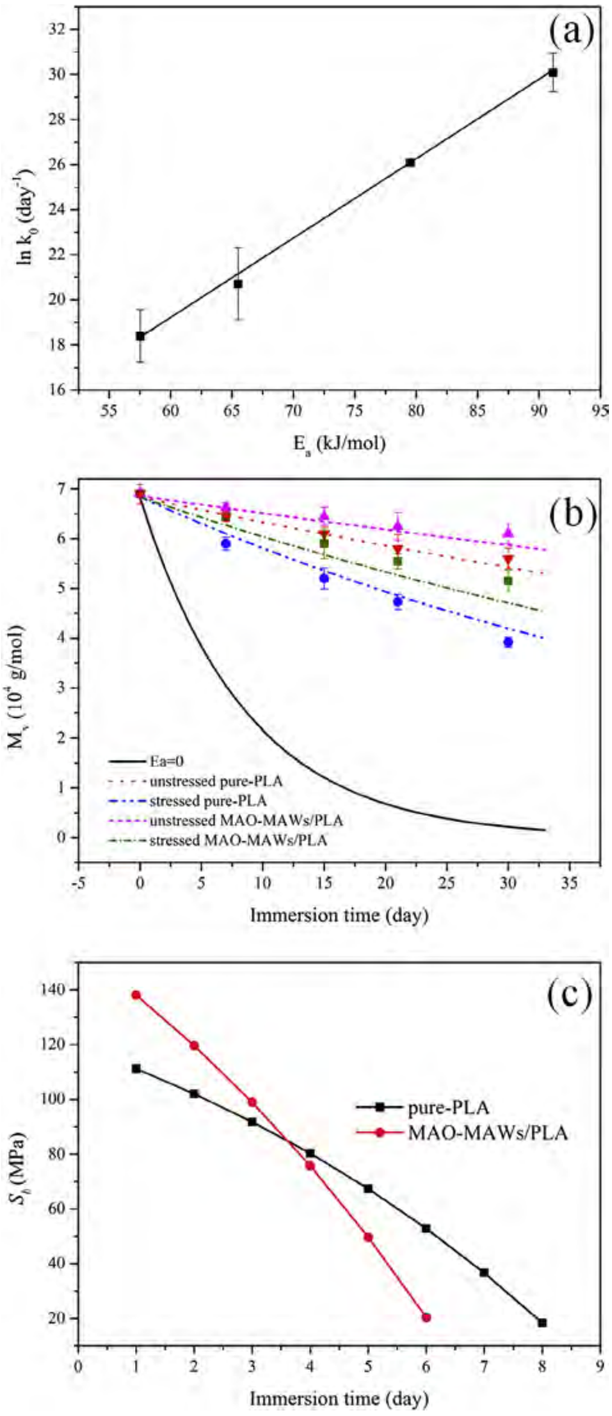

Fig. 10. (a) ln k_0 as a function of E_a, (b) M_v as a function of immersion time at 37 °C and (c) S_b as a function of immersion time for $E_a = 0$.

release and the following diffusion are strongly related to the surface morphologies and distribution of MAO-MAWs. Commonly, pores on the surface of MAO coating would enhance the degradation of MAWs and the production of hydroxide ions. In this work, PLA matrix would penetrate into the pores and then self-seal the pores, reducing the effects of the pores on the degradation of MAWs. The released hydroxide ions could neutralize the acidic ions and then increase the pH. However, if the pH exceeds 7.8, it would break the balance of pH depended physiological reactions [41,42]. Whereas in the alkaline solution, hydrolytic degradation of PLA would be accelerated [43], on the other hand retarding the rising of pH. The synergic reaction between the two components stabilizes pH to be a steady value at 37 °C.

Moreover, it could be noticed that PLA matrix in the composite has a lower degradation rate than that of pure-PLA. The question is how MAO-MAWs mitigate the degradation of PLA. One assumption is due to the function of the neutralization, which maintains the pH to be neutral. This assumption is on the basis that the degradation rate or the autocatalytic degradation rate depends on the presence of H^+. However, a study performed by Schliecker et al. [44] shows that the lowest degradation rate appeared around pH 4.5 rather than pH 7.4 for D,L-lactic acid, indicating pure-PLA should have a lower degradation rate. Another systematical study by Lyu et al. [17] denotes that the hydrolysis rate and the autocatalytic reaction depends on the presence of the carboxylic acid groups(–COOH), but not H^+. In this respect, the possible mechanism for the mitigation is due to the interaction between Mg^{2+} ions released by the degradation of Mg fillers and the carboxylic acid groups from the degradation of PLA matrix, which probably forms inter- or intramolecular crosslinks [45,46]. This assumption could be further supported by the complexion of Mg^{2+} ions to polyesters [47–50]. Such interaction would probably decrease the solubility of PLA matrix [45] as well as the concentration of the carboxylic acid groups, and then reduce the degradation rate or autocatalytic reaction rate. As a result, the interaction between MAO-MAWs and PLA could be described as follows: water molecules firstly penetrate into PLA, triggering hydrolytic degradation of the ester linkage and forming acidic carboxyl end groups. As time elapses, water molecules diffuse through PLA matrix and attack MAO-MAWs, causing the degradation of MAO coating. Thereafter, cracks would emerge locally and partially expose the MAWs substrate. Degradation of the MAO coating or the MAW substrate would release hydroxide ions and Mg^{2+} ions. The former alkaline ions counteract the pH decrease to maintain a steady value, while the later Mg^{2+} ions react with –COOH to mitigate the degradation of PLA matrix. The main mechanism is schematically depicted in Fig. 11.

3.3.3. Effects of immersion temperature

Obviously, increasing immersion temperature significantly raises the degradation rate of PLA and the composite. The temperature effect on the degradation rate of PLA, as well as the correlation between normal and accelerated tests for pure-PLA and the composite could be quantitatively conducted according to the degradation kinetics of PLA. This offers a basis for the design of accelerated tests, involving the selection of immersion temperature and time to reflect the normal tests under specific immersion time. However, it should be mentioned that the studied immersion temperature in this work is below the glass transformation temperature (T_g) of PLA. As the immersion temperature increases to above T_g, degradation kinetics, as well as the properties of PLA would have a change [17]. Thus, the immersion temperature based on the degradation kinetics proposed in this work should not exceed T_g. Additionally, as mentioned above, the degradation of MAO-MAWs in the composite is strongly related to the diffusion of water molecules through PLA matrix. While the immersion temperature increases, this diffusion would be promoted and then the degradation of MAO-MAWs is accelerated, resulting in the increase of pH value of the solution and the mass loss of the composite.

3.3.4. Effects of compression stress

In mechanochemistry, the following modified Arrhenius equation [51,52] is commonly used to quantitatively evaluate the influence of stress on the stressed polymers:

$$k_b = k_f \exp[-(E_0 - \alpha\sigma)/RT] \tag{11}$$

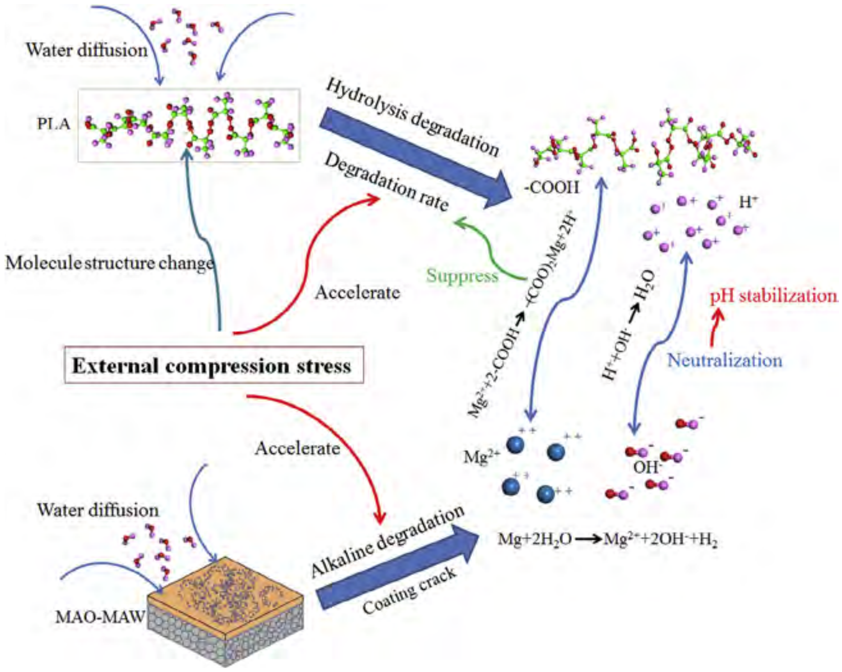

Fig. 11. Schematic illustration of the synergistic degradation effects rendered by the Mg fillers and external compression stress on the degradation kinetics of PLA matrix in the composite.

where k_f is the Arrhenius frequency factor, k_b is the rate of bond-rupture events, E_0 is the activation energy of the static sample, σ is the external stress value, and α is the coefficient. Here, the external stress is considered to alter the reaction rate by changing the activation energy, while the Arrhenius frequency factor is constant. However, according to our study, k_f varies from the activation energy. It has been reported that external stress reduces the activation energy and pre-exponential factor thereby accentuating and inhibiting the chemical reaction in stressed elastomers, respectively [53]. Thus, the pre-exponential factor is also influenced by the external stress. If stress affects the activation energy in Eq. (11), the relationship between σ and activation energy (E_a) can be described as follows:

$$E_a = E_0 - \alpha\sigma \tag{12}$$

where α is the coefficient calculated to be 2.2×10^{-5} kJ/(mol·Pa) Then, σ is 3.65 MPa when $E_a = 0$. This result is not reasonable as it is derived based on the assumption of Eq. (11). In fact, Eq. (11) is based on that the structure of the molecule does not change in the reaction, while there would exit stress energy for a unstressed molecule to remain the initial structure unchanged [54]. On the contrary, with regard to PLA, not only the activation energy, but also the molecule structure, may change with the external stress [32,55]. Hence, the external compression stress influences degradation of pure-PLA by changing the activation energy and molecular structure as shown in Fig. 11. Regarding the composite, compression stress also accelerates degradation of MAO-MAWs thereby affecting the neutralizing function and the interaction between Mg^{2+} and –COOH, which would indirectly influence the degradation rate of the PLA matrix.

4. Conclusions

The effects of the immersion temperature and compression stress on the initial *in vitro* degradation kinetics of pure-PLA and the composite reinforced with MAO-MAWs are investigated. The main conclusions could be stated as follows:

(1) The *in vitro* degradation kinetics of the unstressed or stressed pure-PLA and MAO-MAWs/PLA (or Mg/PLA) composite is Arrhenius-like. A linear relationship between activation energy and logarithmic pre-exponential factor is observed and a numerical model is established to elucidate the relationship of the PLA molecular weight, activation energy, immersion time and temperature.
(2) The PLA matrix in MAO-MAWs/PLA composite has a lower degradation rate than that of pure-PLA attributed to the synergic function of Mg^{2+} ions released by the degradation of Mg fillers, which interact with the carboxylic acid groups from the degradation of PLA.
(3) The external compression stress changes the molecular structure of PLA and decreases the activation energy and pre-exponential factor resulting in enhanced degradation of PLA.
(4) There are well-defined relationships between the bending strength of the specimens and the PLA molecular weight during immersion, which are independent of the degradation temperature and external compression stress.
(5) The accelerated tests in which the immersion temperature is increased are valid for the composite and the results can be correlated with those from normal tests based on the degradation kinetics.

Acknowledgements

This work was jointly supported by the National Natural Science Foundation of China (Grant No. 31570961), the State Key Program of National Natural Science Foundation of China (Grant No. 51631003), Scientific Research Foundation of Graduate School of Southeast University (YBJJ1525), Jiangsu Key Laboratory for Advanced Metallic Materials (BM2007204), and Hong Kong Research Grants Council (RGC) General Research Funds (GRF) No. CityU 11301215.

References

[1] K.J.L. Burg, S. Porter, J.F. Kellam, Biomaterial developments for bone tissue engineering, Biomaterials 21 (2000) 2347–2359.

[2] H. Mehboob, S.-H. Chang, Application of composites to orthopedic prostheses for effective bone healing: a review, Compos. Struct. 118 (2014) 328–341.

[3] A.J.R. Lasprilla, G.A.R. Martinez, B.H. Lunelli, A.L. Jardini, R.M. Filho, Poly-lactic acid synthesis for application in biomedical devices — a review, Biotechnol. Adv. 30 (2012) 321–328.

[4] B.D. Ratner, A.S. Hoffman, F. Schoen, J.E. Lemons, Biomaterials Science: An Introduction to Materials in Medicine, Elsevier, San Diego, 2004.

[5] H. Okada, H. Toguchi, Biodegradable microspheres in drug delivery, Crit. Rev. Ther. Drug 12 (1995) 1–99.

[6] J. Suganuma, H. Alexander, Biological response of intramedullary bone to poly-L-lactic acid, J. Appl. Biomater. 4 (1993) 13–27.

[7] M.S. Taylor, A.U. Daniels, K.P. Andriano, J. Heller, Six bioabsorbable polymers: In vitro acute toxicity of accumulated degradation products, J. Appl. Biomater. 5 (1994) 151–157.

[8] X. Li, C.L. Chu, L. Liu, X.K. Liu, J. Bai, C. Guo, F. Xue, P.H. Lin, P.K. Chu, Biodegradable poly-lactic acid based-composite reinforced unidirectionally with high-strength magnesium alloy wires, Biomaterials 49 (2015) 135–144.

[9] Y.H. Wu, N. Li, Y. Cheng, Y.F. Zheng, Y. Han, In vitro study on biodegradable AZ31 magnesium alloy fibers reinforced PLGA composite, J. Mater. Sci. Technol. 29 (2013) 545–550.

[10] R.N. Oosterbeek, C.K. Seal, M.P. Staiger, M.M. Hyland, Topologically ordered magnesium-biopolymer hybrid composite structures, J. Biomed. Mater. Res. A 103 (2015) 311–317.

[11] P. Uppstu, C. Paakki, A. Rosling, In vitro hydrolysis and magnesium release of poly(d, l-lactide-co-glycolide)-based composites containing bioresorbable glasses and magnesium hydroxide, J. Appl. Polym. Sci. 132 (2015) 42646.

[12] Y.F. Zheng, X.N. Gu, F. Witte, Biodegradable metals, Mater. Sci. Eng. R. 77 (2014) 1–34.

[13] H. Liu, R. Wang, H.K. Chu, D. Sun, Design and characterization of a conductive nanostructured polypyrrole-polycaprolactone coated magnesium/PLGA composite for tissue engineering scaffolds, J. Biomed. Mater. Res. A 103 (2015) 2966–2973.

[14] S.C. Cifuentes, R. Gavilán, M. Lieblich, R. Benavente, J.L. González-Carrasco, In vitro degradation of biodegradable polylactic acid/magnesium composites: relevance of Mg particle shape, Acta Biomater. 32 (2016) 348–357.

[15] V. Piemonte, F. Gironi, Kinetics of hydrolytic degradation of PLA, J. Polym. Environ. 21 (2013) 313–318.

[16] F. Codari, S. Lazzari, M. Soos, G. Storti, M. Morbidelli, D. Moscatelli, Kinetics of the hydrolytic degradation of poly(lactic acid), Polym. Degrad. Stab. 97 (2012) 2460–2466.

[17] J. Lyu Schley, B. Loy, D. Lind, C. Hobot, R. Sparer, D. Untereker, Kinetics and time−temperature equivalence of polymer degradation, Biomacromolecules 8 (2007) 2301–2310.

[18] P. Wan, C. Yuan, L. Tan, Q. Li, K. Yang, Fabrication and evaluation of bioresorbable PLLA/magnesium and PLLA/magnesium fluoride hybrid composites for orthopedic implants, Compos. Sci. Technol. 98 (2014) 36–43.

[19] P.C.A. Joziasse, W.D. Grijpma, E.J. Bergsma, W.F. Cordewener, M.R.R. Bos, J.A. Pennings, The influence of morphology on the (hydrolytic degradation of as-polymerized and hot-drawn poly(L-lactide)), Colloid Polym. Sci. 276 (1998) 968–975.

[20] H. Tsuji, A. Mizuno, Y. Ikada, Properties and morphology of poly(L-lactide). III. Effects of initial crystallinity on long-term in vitro hydrolysis of high molecular weight poly(L-lactide) film in phosphate-buffered solution, J. Appl. Polym. Sci. 77 (2000) 1452–1464.

[21] P. Li, X. Feng, X. Jia, Y. Fan, Influences of tensile load on in vitro degradation of an electrospun poly(l-lactide-co-glycolide) scaffold, Acta Biomater. 6 (2010) 2991–2996.

[22] M. Guo, Z. Chu, J. Yao, W. Feng, Y. Wang, L. Wang, Y. Fan, The effects of tensile stress on degradation of biodegradable PLGA membranes: a quantitative study, Polym. Degrad. Stab. 124 (2016) 95–100.

[23] M. Deng, J. Zhou, G. Chen, D. Burkley, Y. Xu, D. Jamiolkowski, T. Barbolt, Effect of load and temperature on in vitro degradation of poly(glycolide-co-l-lactide) multifilament braids, Biomaterials 26 (2005) 4327–4336.

[24] M.J. Gardner, M.C. van der Meulen, D. Demetrakopoulos, T.M. Wright, E.R. Myers, M.P. Bostrom, In vivo cyclic axial compression affects bone healing in the mouse tibia, J. Orth. Res. 24 (2006) 1679–1686.

[25] S. Park, C.T. Hung, G.A. Ateshian, Mechanical response of bovine articular cartilage under dynamic unconfined compression loading at physiological stress levels, Osteoarthritis Cartilage 12 (2004) 65–73.

[26] K.J. Faran, N. Ichioka, M.A. Trzeciak, S. Han, J. Medige, O.J. Moy, Effect of bone quality on the forces generated by compression screws, J. Biomech. 32 (1999) 861–864.

[27] C.L. Chu, X. Han, J. Bai, F. Xue, P.K. Chu, Fabrication and degradation behavior of micro-arc oxidized biomedical magnesium alloy wires, Surf. Coat. Technol. 213 (2012) 307–312.

[28] N.T. Kirkland, N. Birbilis, Magnesium Biomaterials: Design, Testing, and Best Practice, Springer, Switzerland, 2014.

[29] A. Schindler, D. Harper, Polylactide. II. Viscosity–molecular weight relationships and unperturbed chain dimensions, J. Polym. Sci. Pol. Chem. 17 (1979) 2593–2599.

[30] I.M. Ward, J. Sweeney, Mechanical Properties of Solid Polymers, John Wiley & Sons, New York, 2012.

[31] R.E. Bullock, Strength ratios of composite materials in flexure and in tension, J. Compos. Mater. 8 (1974) 200–206.

[32] A.Z. Kharazi, M.H. Fathi, F. Bahmani, H. Fanian, Nonmetallic textile composite bone plate with desired mechanical properties, J. Compos. Mater. 46 (2012) 2753–2761.

[33] F. Bueche, A new class of switching materials, J. Appl. Phys. 44 (1973) 532–533.

[34] J. Vilčáková, P. Sáha, V. Křesálek, O. Quadrat, Pre-exponential factor and activation energy of electrical conductivity in polyester resin/carbon fibre composites, Synth. Met. 113 (2000) 83.

[35] A. Corma, F. Llopis, J.B. Monton, S. Weller, On the compensation effect in acid-base catalyzed reactions on zeolites, J. Catal. 142 (1993) 97–109.

[36] N. Katada, S. Sota, N. Morishita, K. Okumura, M. Niwa, Relationship between activation energy and pre-exponential factor normalized by the number of Bronsted acid sites in cracking of short chain alkanes on zeolites, Catal. Sci. Technol. 5 (2015) 1864–1869.

[37] A. Yildiz, F. Iacomi, M. Cazacu, A. Amironesei, G.I. Rusu, S. Simon, The Meyer-Neldel rule in layered silicone-silver nanocomposites, Polym. Compos. 32 (2011) 1751–1756.

[38] Z. Huang, Q. Ye, L. Teng, A comparison study on thermal decomposition behavior of poly(l-lactide) with different kinetic models, J. Therm. Anal. Calorim. 119 (2014) 2015–2027.

[39] P. Nordström, T. Pohjonen, P. Törmälä, P. Rokkanen, Shear-load carrying capacity of cancellous bone after implantation of self-reinforced polyglycolic acid and poly-l-lactic acid pins: experimental study on rats, Biomaterials 22 (2001) 2557–2561.

[40] O. Böstman, J. Viljanen, S. Salminen, H. Pihlajamäki, Response of articular cartilage and subchondral bone to internal fixation devices made of poly-l-lactide: a histomorphometric and microradiographic study on rabbits, Biomaterials 21 (2000) 2553–2560.

[41] G. Song, Recent progress in corrosion and protection of magnesium alloys, Adv. Eng. Mater. 7 (2005) 563–586.

[42] G. Song, Control of biodegradation of biocompatible magnesium alloys, Corros. Sci. 49 (2007) 1696–1701.

[43] D. Cam, S.-H. Hyon, Y. Ikada, Degradation of high molecular weight poly(l-lactide) in alkaline medium, Biomaterials 16 (1995) 833–843.

[44] G. Schliecker, C. Schmidt, S. Fuchs, T. Kissel, Characterization of a homologous series of d, l-lactic acid oligomers; a mechanistic study on the degradation kinetics in vitro, Biomaterials 24 (2003) 3835–3844.

[45] Y. Zhang, S. Zale, L. Sawyer, H. Bernstein, Effects of metal salts on poly(DL-lactide-co-glycolide) polymer hydrolysis, J. Biomed. Mater. Res. 34 (1997) 531–538.

[46] H. Mobedi, M. Nekoomanesh, H. Orafaei, H. Mivehchi, Studying the degradation of poly(L-lactide) in presence of magnesium hydroxide, Iran. Polym. J. 15 (2006) 31–39.

[47] M. Rimmen, J. Matthiesen, N. Bovet, T. Hassenkam, C.S. Pedersen, S.L.S. Stipp, Interactions of Na+, K+, Mg2+, and Ca2+ with benzene self-assembled monolayers, Langmuir 30 (2014) 9115–9122.

[48] B. Wu, B.J. Duncombe, A.J. Stace, The solvation of Mg2+ with Gas-Phase clusters composed of alcohol molecules, J. Phys. Chem. A 112 (2008) 2182–2191.

[49] S.-K. Yoo, E.S. Awad, M.A. El-Sayed, Comparison between the Binding of Ca2+ and Mg2+ to the Two High-Affinity Sites of Bacteriorhodopsin, J. Phys. Chem. 99 (1995) 11600–11604.

[50] C. De Stefano, A. Gianguzza, D. Piazzese, Complexes of azelaic and diethylenetrioxydiacetic acids with Na+, Mg2+, and Ca2+ in NaCl aqueous solutions, at 25 & #xB0;C, J. Chem. Eng. Data 45 (2000) 15–19.

[51] D.A. Davis, A. Hamilton, J. Yang, L.D. Cremar, D. Van Gough, S.L. Potisek, M.T. Ong, P.V. Braun, T.J. Martinez, S.R. White, J.S. Moore, N.R. Sottos, Force-induced activation of covalent bonds in mechanoresponsive polymeric materials, Nature 459 (2009) 68–72.

[52] M.K. Beyer, H. Clausen-Schaumann, Mechanochemistry: the mechanical activation of covalent bonds, Chem. Rev. 105 (2005) 2921–2948.

[53] N.Y. Rapoport, E.Z. Gennadii, Kinetics and mechanism of the oxidation of polymers in a stressed state, Russ. Chem. Rev. 52 (1983) 897–916.

[54] A.A. Popov, G.E. Zaikov, N.N. Semeriov, Kinetics of chemical reactions of stressed polymers, Int. J. Polym. Mater. 17 (1992) 143–149.

[55] Y. Fan, P. Li, X. Yuan, Influence of mechanical loads on degradation of scaffolds, in: C.T. Lim, J.C.H. Goh (Eds.), 6th World Congress of Biomechanics (WCB 2010) August 1–6, 2010 Singapore: Springer, Berlin Heidelberg, 2010, pp. 549–552.